Equations of state of Rb_xC_{60} ($x=3$, 4, and 6)

A. A. Sabouri-Dodaran, M. Marangolo, Ch. Bellin, F. Mauri, G. Fiquet, and G. Loupias
Laboratoire de Minéralogie et de Cristallographie de Paris-CNRS-Universités Paris VI et VII, IPGP, 4 Place Jussieu, F-75252 Paris Cedex 05, France

M. Mezouar and W. Crichton
European Synchrotron Radiation Facility (ESRF), BP 220, 38043 Grenoble Cedex, France

C. Hérold
Laboratoire de Chimie du Solide Minéral, Université Henri Poincaré Nancy I, Boîte Postale 239, 54506 Vandoeuvre lès Nancy cedex, France

F. Rachdi
Groupe de Dynamique des Phases Condensées UMR5581 CNRS—Université Montpellier II, Place Eugène Bataillon 34095 Montpellier Cedex 5, France

S. Rabii
Department of Electrical Engineering, University of Pennsylvania, Philadelphia, Pennsylvania 19104-6390, USA
(Received 20 April 2004; published 29 November 2004)

The equations of state (EOS) of Rb_xC_{60} ($x=3$, 4, and 6) were determined by high pressure x-ray diffraction measurements. We focus on Rb_4C_{60} since a Mott insulator-metal transition can be induced at around 0.8 GPa. We observed an abrupt jump in the compressibility of Rb_4C_{60} between 0.5 GPa and 0.8 GPa which is attributed to a structural phase transition preserving the tetragonal symmetry. By *ab initio* calculations we are able to reproduce the experimental equations of state of Rb_xC_{60} ($x=3,4$). These calculations permit us to study the pressure dependence of the internal coordinates.

DOI: 10.1103/PhysRevB.70.174114 PACS number(s): 61.48.+c, 61.50.Ks, 71.20.Tx

I. INTRODUCTION

The alkali-doped fullerene compounds A_3C_{60}, A_4C_{60} and A_6C_{60} (A=Rb and K) present different properties. A_3C_{60} are metals and superconductors, A_4C_{60} are insulators, and A_6C_{60} are filled band insulators.[1]

The bct structured A_4C_{60} (Ref. 2) (A=K, Rb) are perhaps the most interesting compounds because they are nonmagnetic narrow-gap insulators[3] that undergo a pressure-induced Mott insulator-metal transition at around 0.8 GPa.[4] Theoretical investigations invoke Coulomb repulsion, orbital degeneracy, and the Jahn-Teller effect[3] to explain their nonmagnetic insulating character rather than the metallic nature expected in a band-structure picture.[5] The main parameters for describing these systems, which are close to a Mott transition, are the Coulomb interaction U between electrons on the same molecule, the band width W, and the critical value $(U/W)_c$ for the insulator-metal transition.[6]

In this article, we present a study of the crystal structure of Rb_nC_{60} ($n=3$, 4, and 6) under pressure. The following points motivated our work: while the Rb_3C_{60} equation of state has been measured by many groups, the Rb_4C_{60} equation of state is unknown despite its great interest due to the Mott transition at 0.8 GPa.[4] In this context, it is very important to know if a structural transition comes with the Mott transition. Moreover, by changing pressure, we can modify the band width W, permitting a rough evaluation of the critical value $(U/W)_c$ around the Mott transition.

It is worthwhile recalling that it is not possible to prepare samples without traces of either fcc A_3C_{60} or bcc A_6C_{60}.[7] This means that x-ray diffraction patterns must be studied very carefully. The measure of A_3C_{60} and A_6C_{60} under the same experimental conditions permit us to determine their contribution to experimental spectra. Moreover, this allows us to compare the compressibility of A_4C_{60} with compressibilities of the other phases. Experimental results are reported in Sec. II.

In Sec. III, by *ab initio* fully relaxed electronic structure calculations we study the Rb_3C_{60} and Rb_4C_{60} equations of state. Moreover, these calculations give an insight into the pressure dependence of the internal coordinates and permit to discuss the Rb_4C_{60} insulator-metal phase transition at around 1 GPa.

II. EXPERIMENTAL DETERMINATION OF THE STRUCTURAL EVOLUTION UNDER PRESSURE

A. Experiment

Diffraction experiments have been performed on two powder samples of Rb_4C_{60}: one from the University of Montpellier (France) (called Rb_4C_{60}-M) and the other from the University of Nancy (France) (called Rb_4C_{60}-N). Diffraction experiments of Rb_3C_{60} have been performed on a powder sample from the University of Nancy. Rb_4C_{60} and Rb_3C_{60} powder were synthesized by first preparing the compound Rb_6C_{60} using a vapor-transport method.[8] Part of the Rb_6C_{60} was then used to prepare Rb_4C_{60} and Rb_3C_{60} by a direct reaction with additional stoichiometric amounts of

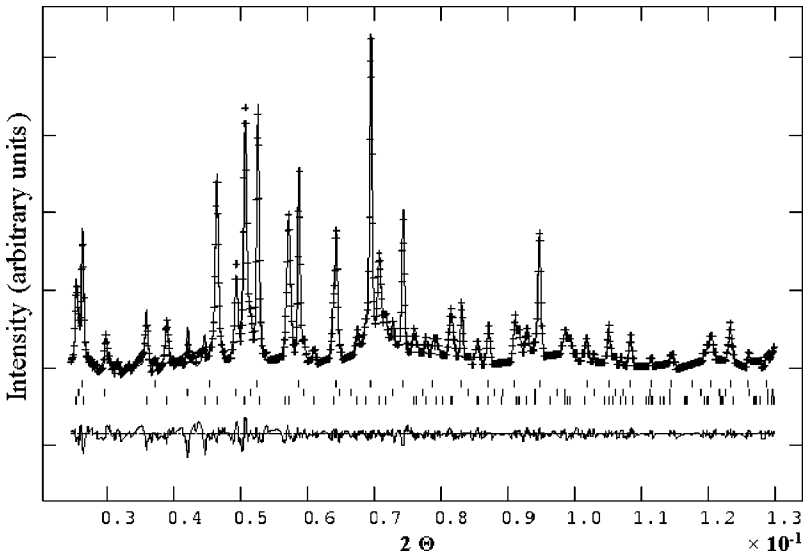

FIG. 1. The Le Bail fit of full structure of a diffraction spectrum of the Rb_4C_{60}-Montpellier sample at room pressure and room temperature without the diamond-anvil cell environment, using a monochromatic beam (0.3738 Å). This sample contains Rb_4C_{60} (lower ticks) space group I4/mmm, $a=11.96$ Å, $c=11.02$ Å and two minor phases: Rb_6C_{60} (upper ticks) space group $Im\bar{3}$; Rb_3C_{60} space group $Fm\bar{3}m$ (middle ticks). The quality of fit is gauged by the weighted profile R factor: $R_{pw}=2.7\%$, $Rp=2.1\%$, $\chi^2=1.4$.

pure C_{60}. All the samples were checked at ambient pressure by x-ray diffraction. Figure 1 shows the patterns from Rb_4C_{60}-M, which exhibits the coexistence of well-defined Rb_3C_{60} and Rb_6C_{60} phases in addition to Rb_4C_{60}.[4,7,9,10]

The x-ray diffraction powder data were obtained at the ID-30 beam line of the European Synchrotron Radiation Facility (ESRF, Grenoble, France) by the angle dispersive x-ray diffraction technique employing monochromatic ($\lambda=0.3738$ Å) radiation. All measurements were carried out at room temperature. In a glove box the samples were loaded in a membrane cell with a diamond culet of diameter 350 μm (Rb_4C_{60}-M and Rb_3C_{60}-N) or 600 μm (Rb_4C_{60}-N).[11]

Pressure values below 5 GPa were measured by using the ruby fluorescence method with a precision of 0.05 GPa. X-ray diffraction patterns were collected in angle-resolved geometry on an image plate detector (Mar345). The sample-to-detector distance and the image plate angles were analyzed using the ESRF Fit2D software,[12] and images subsequently integrated in conventional intensity versus 2θ angle patterns.

B. Results

1. Rb_4C_{60} *and* Rb_6C_{60}

The results of Le Bail fitting are presented in Fig. 1 (Rb_4C_{60}-M) and Fig. 2 (Rb_4C_{60}-N) at room pressure and temperature, with no pressure transmitting medium.

The Rb_4C_{60}-M sample is a three phases assemblage, including (1) Rb_4C_{60}, space group I4/mmm, $a=11.96$ Å, $c=11.02$ Å (Ref. 2); (2) Rb_6C_{60}, space group $Im\bar{3}$, $a=11.54$ Å (Ref. 10); (3) Rb_3C_{60}, space group $Fm\bar{3}m$, $a=14.42\pm0.02$ Å (Ref. 10).

The Rb_4C_{60}-N sample is a three phase assemblage, including Rb_4C_{60}, Rb_3C_{60} and RbOH-H_2O (space group $Cmc2_1$). Some traces of Rb_6C_{60} were detected only for pressures above 1 GPa. In the case of Rb_4C_{60} the best quality diffraction patterns (shown in the following) have been obtained on the sample from Nancy since only two fullerides coexist in the sample. Moreover, it was possible to determine the equation of state of Rb_6C_{60} directly on the Montpellier sample without performing further measurements on a pure

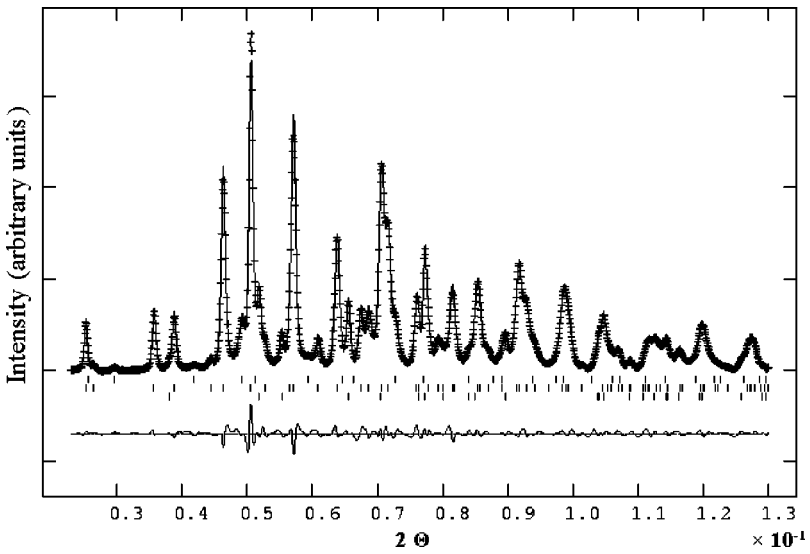

FIG. 2. The Le Bail fit of full structure of a diffraction spectrum of the Rb_4C_{60}-Nancy sample at room pressure and room temperature within the diamond-anvil cell environment, using a monochromatic beam (0.3738 Å). This sample contains Rb_4C_{60} (middle ticks) space group I4/mmm, $a=11.96$ Å, $c=11.02$ Å and two minor phases: Rb_3C_{60} (upper ticks) space group $Fm\bar{3}m$ and RbOH-H_2O space group $Cmc2_1$ (lower ticks).). The quality of fit is gauged by the weighted profile R factor: $R_{pw}=0.92\%$, $Rp=0.58\%$ $\chi^2=0.3$.

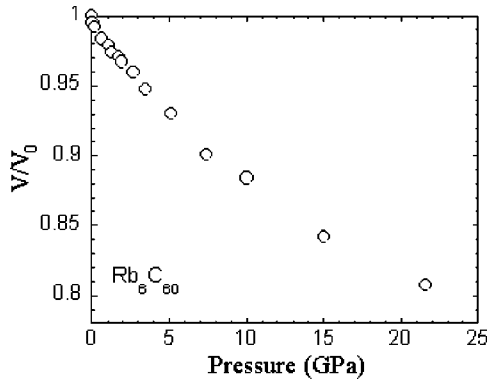

FIG. 3. The Rb_6C_{60} equation of state as obtained by monitoring the minor phase of the Rb_4C_{60}-Montpellier sample.

Rb_6C_{60} sample, since three clear and intense bcc reflections were observed at all the probed pressures. The equation of state of Rb_6C_{60} is shown in Fig. 3.

In order to detect the equation of state of Rb_4C_{60}, data were analyzed using the General Structure Analysis System (GSAS) in the Le Bail configuration:[13] unit-cell parameters, profile shape parameters, and the individual Bragg intensities varied independently. At room temperature and at atmospheric pressure, lattice parameters of Rb_4C_{60} are in agreement with values reported by other groups,[2] i.e. for Rb_4C_{60}, $a=11.96$ Å and $c=11.02$ Å. Since we were successful in fitting spectra by GSAS only at low pressures, lattice parameters above 0.56 GPa were obtained by fitting the position of four peaks of the Rb_4C_{60} bct structure, namely the (200), (301), (103), (222) reflections. Moreover, whenever possible, other reflections were added: (002), (211), (332), (402), and (622). This latter method is corroborated by the analysis of spectra below 0.56 GPa since it gives results identical to those obtained by GSAS. The pressure dependences of three of the four peaks analyzed with this procedure are shown in Fig. 4. At each pressure the position of available reflections could be indexed using the tetragonal unit cell.

The pressure dependences of the lattice parameters (a and c) of Rb_4C_{60} are shown in Fig. 5. We notice that the a parameter decreases almost linearly with pressure. On the other hand, a phase transition preserving the bct structure leads to a jump in c-direction compression and to a contraction in length between 0.56 GPa and 0.8 GPa.

2. Rb_3C_{60}

In the following we will present measurements performed on Rb_3C_{60} samples. Results will be compared with previous measurements obtained before by other groups.[14–16] Our measurements were performed over a more extended pressure range (up to 13 GPa). The Rb_3C_{60} sample was pure and measured using argon as the pressure-transmitting medium. Room temperature diffraction profiles for phase-pure samples of Rb_3C_{60} (the first measurements are at 0.32 GPa) are shown in Fig. 6. As for Rb_4C_{60}, data were analyzed using the General Structure Analysis System (GSAS) in the Le Bail configuration.[13]

Finally, we have compared the equation of state of Rb_3C_{60} with measurements performed by other groups as shown in Fig. 7. Our data match nicely with those obtained by Zhou *et al.*[14] and Diederichs *et al.*[15] On the other hand, data by Ludwig *et al.*[16] give a lower compressibility in comparison with our results, Fig. 7.

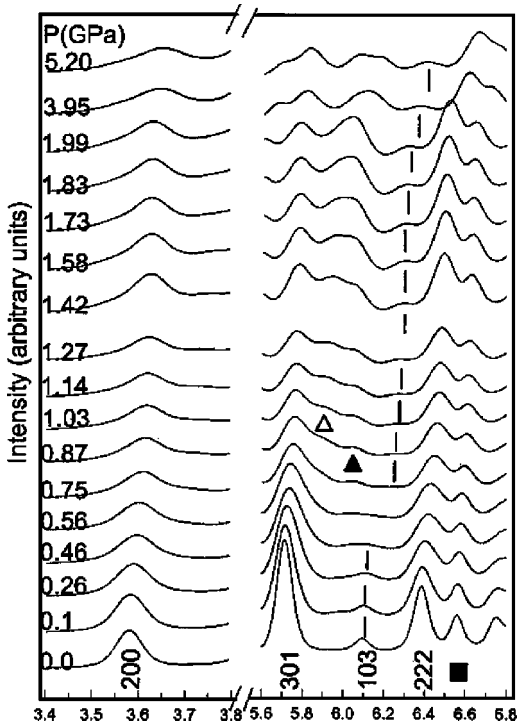

FIG. 4. X-ray patterns for four peaks 200, 301, 103, and 222 of Rb_4C_{60} (tetragonal structure). These peaks were used to obtain the Rb_4C_{60} equation of state. Diffraction peaks of other phases are also observed: The solid square is the (111) reflection of $RbOH\text{-}H_2O$. The solid triangle is the (400) reflection of Rb_3C_{60}. The reflection with the open triangle is attributed to traces of Rb_6C_{60} (reflection (301).

C. Comparison of equations of state of Rb_xC_{60} ($x=3$, 4, and 6)

Since the experimental bulk modulus and its first derivative can be evaluated by different fitting procedures leading to slightly different values, we show in the following the results obtained by three methods: (i) by a linear fit of the

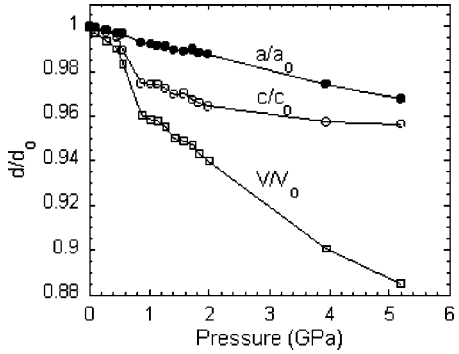

FIG. 5. Rb_4C_{60} under pressure: a/a_0, c/c_0, and V/V_0. A structural phase transition preserving the tetragonal symmetry is observed between 0.56 GPa and 0.8 GPa.

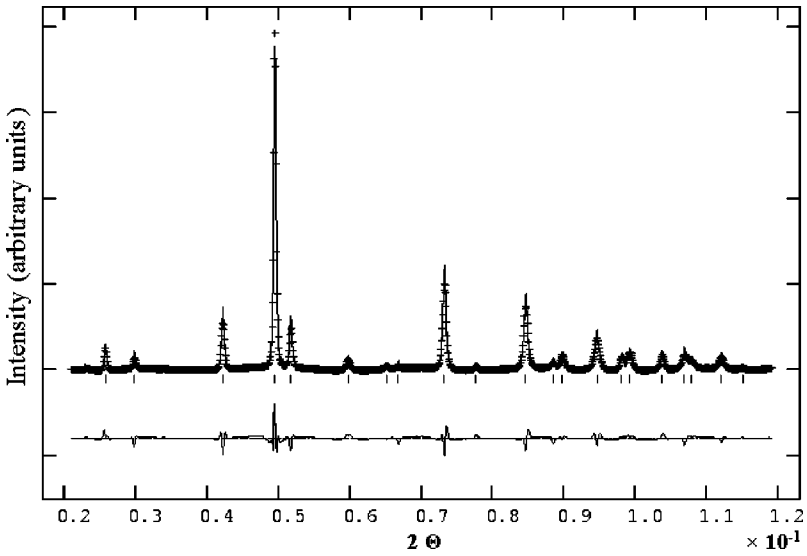

FIG. 6. The Le Bail fit of the full structure of a diffraction spectrum of the Rb_3C_{60} sample at 0.32 GPa and at room temperature within the diamond-anvil cell environment, using a monochromatic beam (0.3738 Å). The space group is $Fm\bar{3}m$ and the lattice parameter $a=14.32$ Å. The quality of fit is gauged by the weighted profile R-factor: gives $R_{pw}=1.02\%$, $Rp=0.59\%$, and $\chi^2=0.2662$.

P(ln V) curve at 0.0–0.5 GPa and at 0.8–1.3 GPa. (ii) By the first order Murnaghan EOS,[17] and (iii) by the Vinet EOS.[18]

Also theoretical B_0 values were calculated using three different methods: (i) by deriving the polynomial fit of the calculated total energy curve $E(V)$ shown in Figs. 8 and 9, i.e., $B_0=V_0(\partial E^2/\partial V^2)_{V0}$. The two other methods exploited the derivative with respect to the volume of the $E(V)$ polynomial curves, i.e. $P(V)$ polynomial curves. These $P(V)$ curves were fitted by (ii) the Vinet's EOS and (iii) by the first order Murnaghan's EOS.

Results are given in Table I. For Rb_3C_{60}, by considering that the cell parameter at room pressure is 14.42 ± 0.02 Å (Ref. 10), we can estimate the bulk modulus between 11.7 ± 1.5 GPa (Vinet methods) and 15.0 ± 2 GPa (linear fit). We notice in Fig. 7 that our points recover data by Diederichs *et al.* even if they found by Murnaghan EOS a bulk modulus of 17.35 ± 0.2 GPa. This is maybe due to the fact that their measurements were performed only up to 0.73 GPa.[15] We notice that Rb_6C_{60} is much less compressible than Rb_3C_{60} (see Table I). A comparison between the free volume of Rb_3C_{60} and Rb_6C_{60} is fruitful: at ambient pressure the free volume of Rb_3C_{60} (the volume of the primitive cell minus the volume of the molecule) is large compared to Rb_6C_{60}, namely 521 $Å^3$ rather than 497 $Å^3$. This can explain the large compressibility of the former compound compared to the latter.

The Murnaghan and Vinet formula[17,18] cannot be used to determine the equation of state of Rb_4C_{60} because of the phase transition at 0.8 GPa. As a consequence, in order to compare the compressibility of the three different compounds and to correlate it with the free volume, we performed a linear fit of the low and high pressure data, below and above the phase transition, taken as separate data (see the first and second columns, Table I). It turns out that at low pressure Rb_3C_{60} is the softest compound and Rb_6C_{60} is the stiffest. Surprisingly, in spite of its large free volume, Rb_4C_{60} is stiffer than Rb_3C_{60} (34.9 GPa and 15.0 GPa, respectively) and it is softer than Rb_6C_{60} (55 GPa). Above the phase tran-

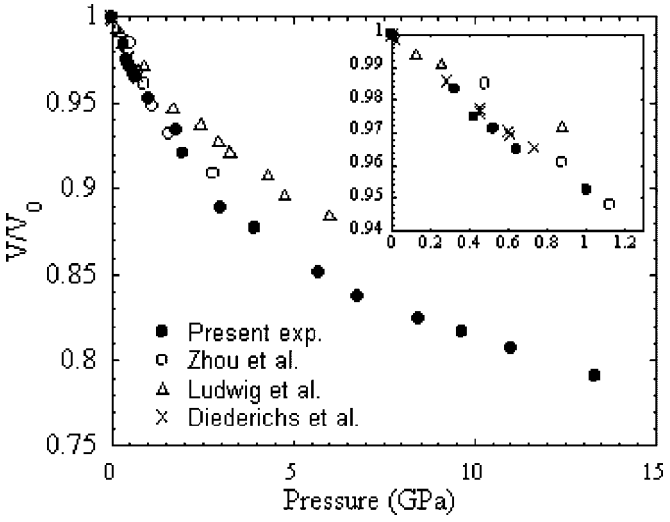

FIG. 7. The Rb_3C_{60} equation of state (present experiments) is compared with data obtained previously by other groups.

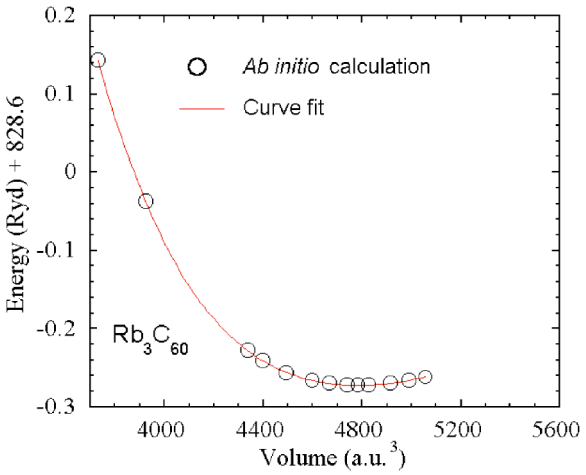

FIG. 8. Rb_3C_{60} Calculated total energy versus volume. The continuous line is a fit of the calculated E(V) points by a fourth degree polynomial.

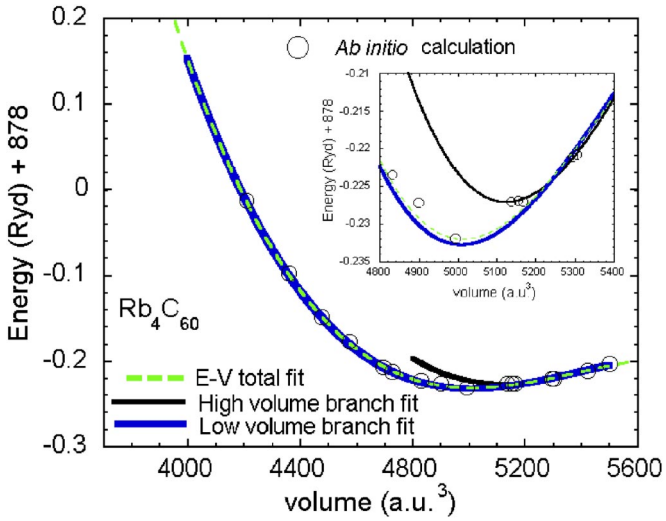

FIG. 9. (Color online) Rb_4C_{60} total energy versus volume. The continuous line is a fit of the calculated $E(V)$ points by a third degree polynomial. Continuous lines (black and blue) correspond to parabolic fits of the high and low volume branches of $E(V)$. The yellow dashed line is a fit of the calculated $E(V)$ points by a third degree polynomial.

sition, at 1 GPa, Rb_4C_{60} stiffens further (72.8 GPa). This is due to the sudden free volume reduction at the phase transition, i.e. from 547.4 Å^3 to 516.2 Å^3.

In the next section we will present the results of the *ab initio* calculations performed on Rb_4C_{60}. Since diffraction spectra were too complex to be analyzed by Rietveld refinement, calculations were performed in order to overcome this difficulty and to give an insight into the pressure dependence of the internal coordinates of Rb_4C_{60}. Moreover, the bandwidth of the conduction band of Rb_4C_{60} was evaluated in order to extract the pressure dependence of the U/W ratio and discuss the insulator-metal phase transition at around 1 GPa.

III. Rb_xC_{60} ($x=3$ and 4): THEORETICAL DETERMINATION OF THE STRUCTURAL EVOLUTION UNDER PRESSURE

A. LDA Band-structure calculations

We obtain the electronic structures and the theoretical equations of state of Rb_xC_{60} ($x=3$ and 4) within density functional theory in the local density approximation, as implemented in the PARATEC code.[19,20] We use norm-conserving pseudo-potentials[21] and we expand in plane waves using a 60 Ry cut off. By increasing the cut off to 80 Ry we found that the forces changed less than 1.8 10^{-4} Ry/a.u. and stress less than 0.08 GPa.

For the pseudopotential generation we use the $2s^2 2p^2$ valence-atomic-configuration for carbon and the $4s^2\ 4p^6\ 4d^0$ configuration rubidium, i.e., we consider 4*s*, 4*p*, and 4*d* as valence states. Within DFT-LDA both materials are metallic with a small conduction band dispersion of approximately 0.5 eV. However, conduction electrons represent only 1/60 of total C_{60} valence electrons. For the BZ integration we use

TABLE I. A comparison of the experimental compressibility values $B=-dP/d(\ln V)$, its derivative $B_0'=dB/dP$ and free volume per C_{60} (Å^3) between Rb_4C_{60}, Rb_3C_{60}, and Rb_6C_{60} B_0 and B_0' in the last two columns are calculated by the Vinet and Murnaghan equations. Experimental B_0 in the first column are obtained by a linear fit of the $P(\ln V)$ curve between 0.0 GPa and 0.5 GPa. To calculate B in the second column we used the same method between 0.8 and 1.2 GPa. Theoretical B_0 and B in the first and second columns are obtained by the derivative of the curve polynomial $E(V)$ fit calculated at 0 GPa and 1 GPa.

	B_0 (GPa) linear Between 0.0–0.5 GPa	B (GPa) linear Between 0.80–1.3 GPa	Free volume per C_{60} (Å^3) at room pressure	Free volume per C_{60} (Å^3) at 0.8 GPa	B_0 (GPa) (Murnaghan)	B_0' (Murnaghan)	B_0 (GPa) (Vinet)	B_0' (Vinet)
Rb_3C_{60} (Exp.)	15.0±2 (linear)	34.83 (linear)	520.6	486.9	13.65±1.2	10.0±0.3	11.7±1.5	13.7±0.6
Rb_4C_{60} (Exp.)	34.9±2 (linear)	72.86 (linear)	547.4	516.2	—	—	—	—
Rb_6C_{60} (Exp.)	52.4±4 (linear)	62.55 (linear)	497.2	482.9	55.4±1.7	5.13±0.3	54±2	6.0±0.4
Rb_4C_{60} (Theor.)	34.7 (polynomial fit *E-V* high volume branch)	39.5 (polynomial fit *E-V* low volume branch)	518.5	483.1	—	—	—	—
Rb_6C_{60} (Theor.)	28.85 (polynomial total fit *E-V*)	39.05 (polynomial total fit *E-V*)	500.1	482.4	40.55±0.06	3.3±0.01	39.15±0.6	3.93±0.015
Rb_3C_{60} (Theor.)	22.49 (polynomial fit *E-V*)	30.87 (polynomial fit *E-V*)	480.2	457.8	16.3±0.04	6.66±0.01	23±0.5	9.0±0.2

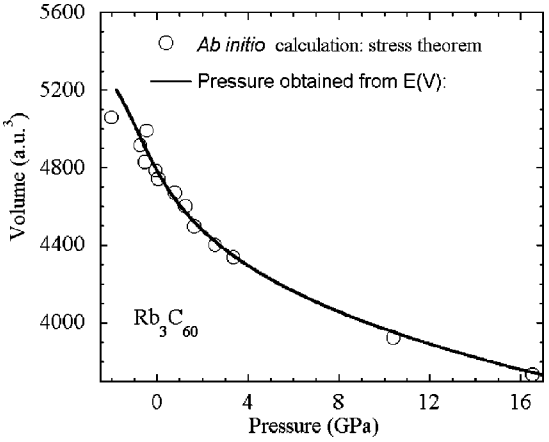

FIG. 10. $V(P)$ points calculated by Nielsen and Martin theorem (open circles) lie on the V(P) curve obtained by the derivative of the $E(V)$ curve of Fig. 8. Negative pressure calculations are obtained by applying a tensile pressure.

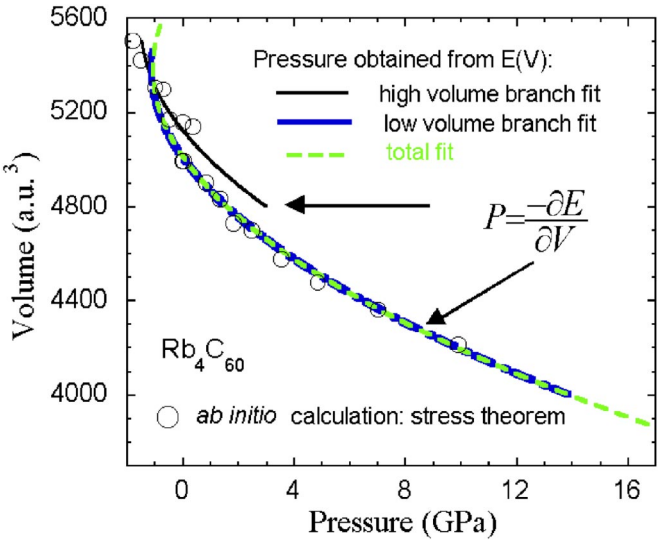

FIG. 11. (Color online) $V(P)$ points calculated by the Nielsen and Martin theorem (open circles) lie on the $V(P)$ curve obtained by the derivative (i) of the total fit of the $E(V)$ curve (the dashed line in Fig. 9) and (ii) of the two $E(V)$ branches (continuous lines in Fig. 9). Negative pressure calculations are obtained by applying a tensile pressure.

a Gaussian smearing of 0.2 eV[22] and a $2\times2\times2$ Monkhorst-Pack grid (4 inequivalents k-points). The use of larger k-point meshes has a very minor effect of the structural parameters.[23]

Rb_3C_{60} has a cubic cell, thus at a given volume the only free parameters are the internal coordinates. For different values of the volume we have minimized the total energy until the forces on atoms were smaller than ~0.002 Ry/a.u. Rb_4C_{60} presents two kinds of free parameters at a given volume: the internal coordinates and the c/a ratio. For different values of the volume we have minimized the total energy until the forces on atoms were smaller than 0.002 Ry/a.u. and the nonhydrostatic components of stress computed using the Nielsen and Martin theorem[24] were less than ~0.1 GPa.

We did not include a possible merohedral disorder effect,[6,25,26] but fixed the C_{60} molecules in the most symmetric configuration (standard orientation),[1] i.e., three double bonds are perpendicular to <100> directions and <111> directions pass through centers of hexagons. In the case of Rb_4C_{60} this choice induces an artificial orthorhombic relaxed structure with a small difference between a and b parameters (less than 0.04 Å).

In Figs. 8 and 9 we show the $E(V)$ curves calculated for Rb_3C_{60} and Rb_4C_{60}. The $E(V)$ curves have been fitted by polynomials (the third and fourth degree polynomials for Rb_3C_{60} and Rb_4C_{60}, respectively). In the case of Rb_4C_{60}, we also fitted the calculated $E(V)$ points by two different branches, i.e. a low pressure branch (or high volume branch) and a high pressure branch (or low volume branch); see continuous lines in Figs. 9 and 11. We notice that the high pressure branch in Fig. 9 cannot be distinguished from the total fit curve.

In Figs. 10 and 11 we plot $V(P)$ curves, obtained by the calculation of the $E(V)$ derivative, i.e. $P=-\partial E/\partial V$, and calculated $V(P)$ points obtained using the Nielsen and Martin theorem. If minimization with respect to internal coordinates is achieved, the two coincide. An overall agreement is found for both materials. In the case of Rb_4C_{60} the agreement is better for $P>2$ GPa. At low pressures the double fitting procedure, i.e. the low and high pressures branch, seems to match better with Nielsen and Martin theorem calculated points. This seems to support an isostructural phase transition, as observed experimentally.

Now, we focus on the comparison between experimental and theoretical results. In Fig. 12 we notice that for both

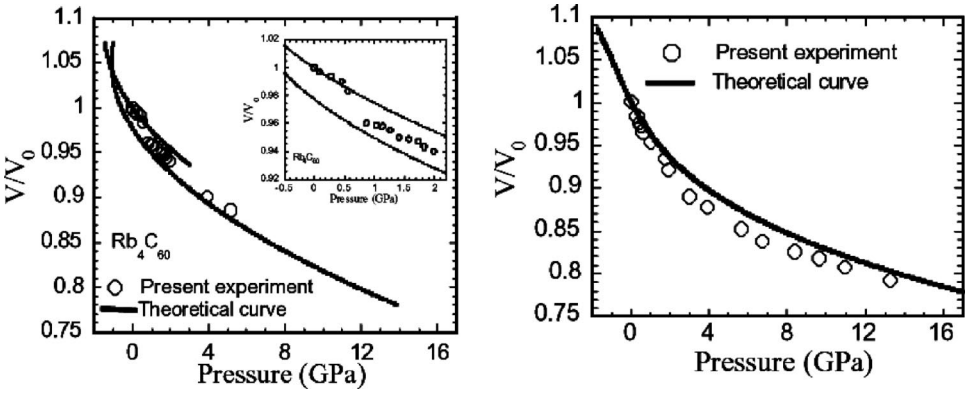

FIG. 12. A comparison of experimental and theoretical equations of state: (a) Rb_3C_{60} and (b) Rb_4C_{60}. Negative pressure calculations are obtained by applying a tensile pressure.

materials we obtain an overall agreement between experimental and calculated equations of states. Calculated bulk moduli, given in Table I, corroborate experimental findings: at ambient pressure Rb_4C_{60} is stiff (34.7 GPa) and Rb_3C_{60} is softer (22.49 GPa), as obtained by the polynomial procedure discussed above.

B. Discussion

1. Rb_4C_{60}: *Pressure dependence of the relaxed atomic positions*

Since calculations on Rb_4C_{60} suggest a possible phase transition close to ambient pressure, as observed experimentally, we looked at the pressure dependence of the calculated relaxed atomic positions in the unit cell. The reader must consider that a comparison with the experimental findings is not straightforward since we did not include the possible merohedral disorder effect that can affect the molecule distortion and the Rb atoms' position.

Concerning carbon atoms, the C_{60} molecule lying in the tetragonal structure is stretched by pressure to become more oblate. Already at ambient pressure, the C_{60} molecule presents an oblate shape: the difference between the long (along the *a* direction) and the short (along the *c*-direction) axes is around 0.03 Å. At 1 GPa the difference between the long (along the *a* direction) and the short (along the *c* direction) axes increases to around 0.05 Å.

Concerning rubidium atoms, we notice that, in the standard orientation, relative to a given C_{60} molecule, the 16 nearest-neighbor alkali atoms can be grouped in four groups.[27] Rb atoms sit (1) symmetrically above a pentagon; (2) strongly asymmetrically above a pentagon; (3) strongly asymmetrically above a hexagon; (4) weakly asymmetrically above a hexagon. In Fig. 13, we report the figures for each group. Two groups of Rb (groups II and III, strongly asymmetric) only have one radial movement in front of the hexagon and pentagon under pressure (Fig. 14). The two other groups (groups I and IV) not only move radially but also tangentially in front of the hexagon and pentagon (Fig. 14). Figure 14 shows that this tangential movement is activated at 0.5 GPa. This phenomenon could be responsible for the abrupt jump in the experimental compressibility of Rb_4C_{60} between 0.56 GPa and 0.8 GPa.

In our calculations we find that Rb-atoms migrate under pressure preserving the symmetries of the space group, as the initial Rb-position for all four groups is determined by Fleming *et al.*[2] $(z, 0.5, 0.0)a$ with $z=0.22$ at room pressure. The evolution of the *z*-parameter is given in Fig. 15. We notice that at 15.0 GPa the value of this parameter is 0.195.

2. Rb_4C_{60}: *Pressure dependence of the bandwidth*

In the inset of Fig. 16 we show the evolution of the t_{1u}-derived bands as a function of the pressure. At atmospheric pressure *W* is around 0.45 eV. At 1 GPa, close to the insulating-metal transition, *W* is around 0.5–0.55 eV, increasing to 0.73 eV at 5 GPa. As expected, *W* depends mainly on lattice parameters *a* and *c*. Indeed, we recalculated *W* at atmospheric pressure, 0.8, 1.9, and 5 GPa by changing the shape of the molecule or the positions of Rb atoms (low pressure atomic positions were introduced in the high pressure unit cell and *vice-versa*). The conclusion is that the influence on the band-width of Rb-atoms positions in the cell and the shape of the C_{60} molecule is negligible.

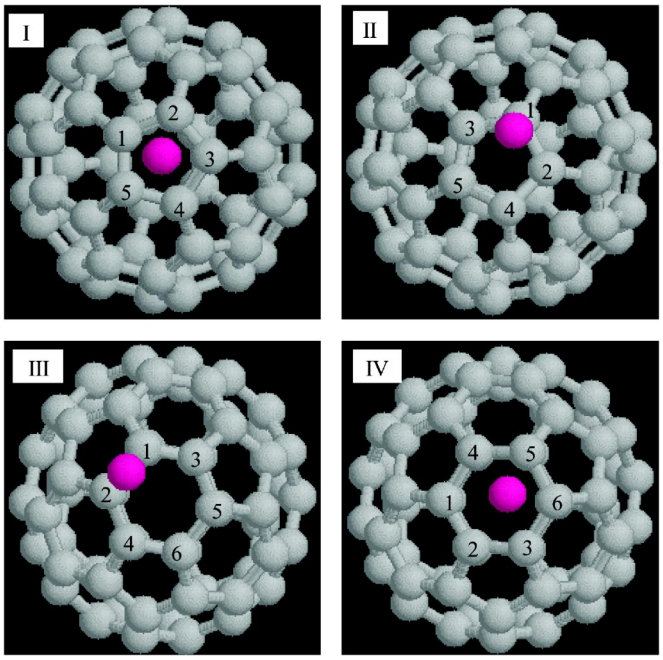

FIG. 13. (Color online) In the standard orientation, relative to a given C_{60} molecule, the 16 nearest-neighbor alkali atoms can be grouped in four groups (Ref. 23). Rb atoms sit (a) symmetrically above a pentagon; (b) strongly asymmetrically above a pentagon, being much closer to one of the pentagon atoms; (c) strongly asymmetrically above a hexagon, being much closer to two of the hexagon atoms; (d) weakly asymmetrically above a hexagon. Notice that nearest neighbor C atoms have been numbered.

The relevant quantity for the insulator-metal transition is the U/W ratio. Other authors have measured and calculated *U* at atmospheric pressure. The calculated value of *U* by Pederson *et al.*[28] is around 1.3 eV, while Antropov *et al.*[29] obtained lower and upper bounds of 0.8 and 1.3 eV, respectively. Lof *et al.*,[30] using Auger spectroscopy, measured 1.6 ± 0.2 eV. Brühwiller *et al.*,[31] using the same technique, obtained 1.4 ± 0.2 eV for this quantity. In Fig. 16, we plot the U/W ratio taking $U=1.3$ eV, independent of the external pressure. Since the insulator-metal transition occurs at around 1 GPa, we can extrapolate to obtain the value of ~ 2.5 for the critical ratio $(U/W)_C$. If we had considered that $U=0.8$ eV, we would have obtained $(U/W)_C$ of ~ 1.5. These estimates are relevant for a comparison with recent theories about the magnetic Mott insulator state of Rb_4C_{60}.

Han *et al.*[32] and Capone *et al.*[33] have applied the dynamical mean-field theory (DMFT) to understand why A_4C_{60} is an insulator. The former study concluded that the cubic structure favors A_3C_{60} being a metal $[(U/W)_C \sim 2.5]$ while the tetragonal structure leads to A_4C_{60} being an insulator $[(U/W)_C \sim 1.3]$. Capone *et al.* proposed that (i) electron correlations drive the Mott insulating state, while a Jahn-Teller distortion makes the ground state a singlet and (ii) that the $(U/W)_C$ critical value is 0.9–1.0. As a result of our measure-

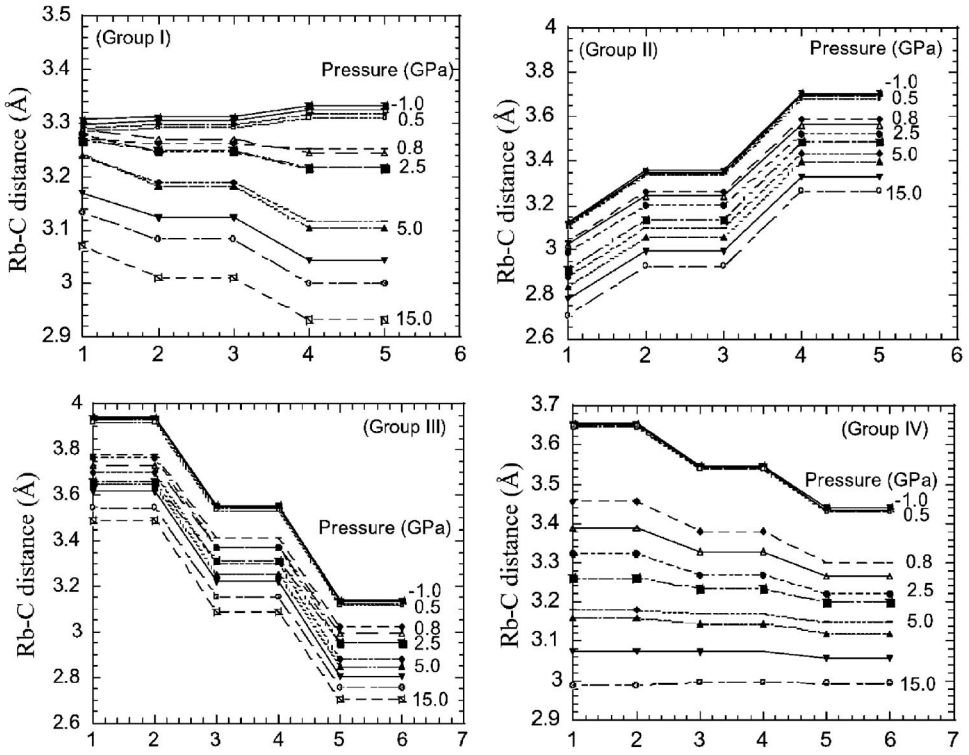

FIG. 14. The pressure induced displacement of four groups of rubidium atoms relative to the pentagon and hexagon faces. All carbon atoms in front of rubidium have been numbered in Fig. 13.

ments and calculations we conclude that these values (0.9–1.3) belong to the very lower bound of critical values. Indeed, if we suppose that U does not vary strongly between 0 and 2 GPa, we have to lower its value to less than 0.7 eV in order to be consistent with the theoretical $(U/W)_C$ critical values.

IV. CONCLUSIONS

We have determined the equation of state of Rb_xC_{60} ($x=3$, 4, and 6) using high pressure x-ray diffraction. We find that Rb_6C_{60} is much less compressible than Rb_3C_{60}. This can be due to the fact that the free volume of Rb_3C_{60} (the volume of the primitive cell minus the volume of the molecule) is large compared to Rb_6C_{60}. On the other hand, it turns out that Rb_4C_{60} is very stiff, in spite of its large free volume. Moreover, at around 1 GPa, an abrupt jump of the compressibility due to a phase transition is detected. This phase transition preserves the tetragonal unit cell symmetry.

For Rb_3C_{60} and Rb_4C_{60}, we find a good agreement between the *ab initio* calculated and the measured equations of state. Moreover, calculations suggest a volume instability at low pressures. We speculate that a rubidium atoms displacement in the unit cell can be at the origin of the calculated volume instability.

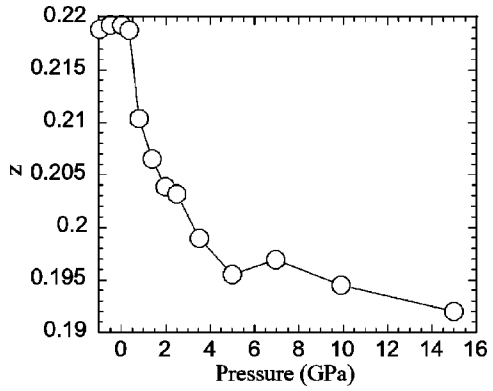

FIG. 15. Atomic position of first group Rb atoms in the tetragonal unit cell. The C_{60} molecule sits at the origin.

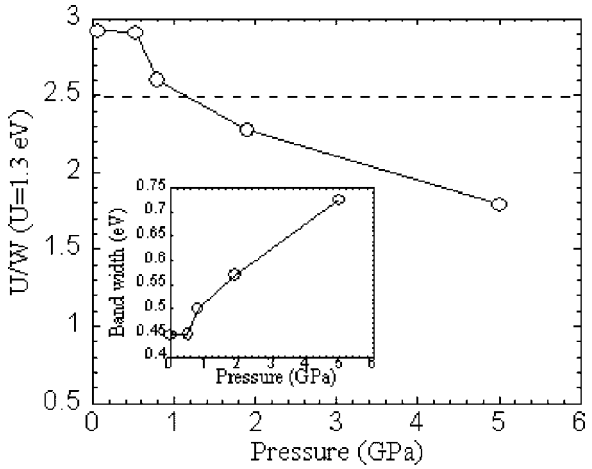

FIG. 16. Pressure dependence of the U/W ratio taking $U=1.3$ eV after calculations of the width of t_{1u}-derived band (inset). The U/W critical value is around 2.5 if we consider that the insulator metal transition happens at around 1 GPa.

By these calculations we also evaluated the band-width of the conduction band of Rb_4C_{60}. This permits us to speculate about the critical ratio $(U/W)_C$ at the Mott transition. Considering that (i) the insulator-metal transition happens at around 1 GPa and that (ii) the lower and upper bounds for U are 0.8 eV and 1.3 eV, the critical ratio $(U/W)_C$ can be estimated to be between 1.5 and 2.5.

ACKNOWLEDGMENTS

We would like to thank E. Tosatti, M. Calandra, A. Shukla, and V. Brouet for helpful discussions. "*Institut du Développement et des Ressources en Informatique Scientifique*" (IDRIS-France) is gratefully acknowledged for calculations performed by an IBM computer.

[1] S. C. Erwin, in *Buckminsterfullerenes*, edited by W. E. Billups and M. A. Ciufolini (VCH, New York, 1993), p. 217 (1993).
[2] R. M. Fleming, M. J. Rossiensky, A. P. Ramirez, D. W. Murphy, J. C. Tully, R. C. Haddon, T. Siegrist, R. Tycko, S. H. Glarum, P. Marsh, G. Dabbagh, S. M. Zahurak, A. V. Makhija, and C. Hampton, Nature (London) **352**, 701 (1991).
[3] M. Fabrizio and E. Tosatti, Phys. Rev. B **55**, 13465 (1997).
[4] R. Kerkoud, P. Auban-Senzier, D. Jérome, S. Brazòvskii, I. Luk'Yanchuk, N. Kirova, F. Rachdi, and C. Goze, J. Phys. Chem. Solids **57**, 143 (1996).
[5] S. C. Erwin and M. R. Pederson, Phys. Rev. Lett. **67**, 1610 (1991).
[6] J. E Han, E. Koch, and O. Gunnarsson, Phys. Rev. Lett. **84**, 1276 (2000).
[7] C. A. Kuntscher, G. M. Bendele, and P. W. Stephens, Phys. Rev. B **55**, R3366 (1997).
[8] A. F. Hebard, M. J. Rosseinsky, R. C. Haddon, D. W. Murphy, S. H. Glarum, T. T. M. Palstra, A. P. Ramirez, and A. R. Kortan, Nature (London) **350**, 600 (1991).
[9] J. Reichenbach, F. Rachdi, I. Luk'yanchuk, M. Ribet, G. Zimmer, and M. Mehring, J. Chem. Phys. **101**, 4585 (1994).
[10] Q. Zhu, O. Zhou, N. Coustel, G. B. M. Vaughan, J. P. McCauley, Jr, W. J. Romanow, J. E. Fischer, and A. B. Smith III, Science **254**, 545 (1991).
[11] J. C. Chervin, B. Canny J. M. Besson, and P. Pruzan, Rev. Sci. Instrum. **66**, 2595 (1995).
[12] D. P. Hammersley, S. O. Svensson, M. Hanfland, A. N. Fitch, and D. Hausermann, High Press. Res. **14**, 235 (1996).
[13] A. Le Bail, H. Duroy, and J. L. Fourquet, Mater. Res. Bull. **23**, 447 (1988).
[14] O. Zhou, G. B. M. Vaughan, Q. Zhu, J. E. Fischer, P. A. Heiney, N. Coustel, J. P. McCauley Jr., and A. B. Smith III, Science **255**, 833 (1992).
[15] J. Diederichs, J. S. Schilling, K. W. Herwig, and W. B. Yelon, J. Phys. Chem. Solids **58**, 123 (1997).
[16] H. A. Ludwig, W. H. Fietz, F. W. Hornung, K. Grube, B. Renker, and G. Burckhard, Physica C **234**, 45 (1994).
[17] F. D. Murnaghan, Am. J. Math. **49**, 235 (1937).
[18] P. Vinet, J. Ferrante, J. H. Rose, and J. R. Smith, J. Geophys. Res. **92**, 9319 (1987).
[19] PARAllel Total Energy Code, B. Pfrommer, D. Raczkowski, A. Canning, and S. G. Louie. With contributions from F. Mauri, M. Cote, Y. Yoon, C. Pickard, and P. Haynes.
[20] B. G. Pfrommer, J. Demmel, and H. Simon, J. Comput. Phys. **150**, 287 (1999); B. G. Pfrommer, M. Coté, S. G. Louie, and M. L. Cohen, *ibid.* **131**, 233 (1997).
[21] N. Troullier and J. L. Martins, Phys. Rev. B **43**, 1993 (1991).
[22] C.-L. Fu and K.-M. Ho, Phys. Rev. B **28**, 5480 (1983).
[23] W. Andreoni, P. Giannozzi, and M. Parrinello, Phys. Rev. B **51**, 2087 (1995).
[24] O. H. Nielsen and R. M. Martin, Phys. Rev. Lett. **50**, 697 (1983); Phys. Rev. B **32**, 3780 (1985); **32**, 3792 (1985).
[25] L. F. Chibotaru, A. Ceulemans, and S. P. Cojocaru, Phys. Rev. B **59**, R12 728 (1999).
[26] O. Gunnarsson, E. Koch, and R. M. Martin, Phys. Rev. B **54**, R11 026 (1996); E. Koch, O. Gunnarsson, and R. M. Martin, Phys. Rev. Lett. **83**, 620 (1999).
[27] O. Gunnarsson, S. C. Erwin, E. Koch, and R. M. Martin, Phys. Rev. B **57**, 2159 (1998).
[28] M. R. Pederson and A. A. Quong, Phys. Rev. B **46**, 13584 (1992).
[29] V. P. Antropov, O. Gunnarsson, and O. Jepsen, Phys. Rev. B **46**, 13647 (1992)
[30] R. W. Lof, M. A. van Veenendaal, B. Koopmans, H. T. Jonkman, and G. A. Sawatzky, Phys. Rev. Lett. **68**, 3924 (1992).
[31] P. A. Brühwiler, A. J. Maxwell, A. Nilsson, N. Martensson, and O. Gunnarsson, Phys. Rev. B **48**, 18296 (1992).
[32] J. E Han, E. Koch, and O. Gunnarsson, Phys. Rev. Lett. **84**, 1276 (2000).
[33] M. Capone, M. Fabrizio, P. Giannozzi, and E. Tosatti, Phys. Rev. B **62**, 7619 (2000).